

# PCCP

Accepted Manuscript



This is an *Accepted Manuscript*, which has been through the Royal Society of Chemistry peer review process and has been accepted for publication.

*Accepted Manuscripts* are published online shortly after acceptance, before technical editing, formatting and proof reading. Using this free service, authors can make their results available to the community, in citable form, before we publish the edited article. We will replace this *Accepted Manuscript* with the edited and formatted *Advance Article* as soon as it is available.

You can find more information about *Accepted Manuscripts* in the [Information for Authors](#).

Please note that technical editing may introduce minor changes to the text and/or graphics, which may alter content. The journal's standard [Terms & Conditions](#) and the [Ethical guidelines](#) still apply. In no event shall the Royal Society of Chemistry be held responsible for any errors or omissions in this *Accepted Manuscript* or any consequences arising from the use of any information it contains.

## COMMUNICATION

# Highly Oriented Large-Scale TIPS Pentacene Crystals and Transistors by Marangoni Effect-Controlled Growth Method

Cite this: DOI: 10.1039/x0xx00000x

Haoyan Zhao,<sup>a</sup> Zhao Wang,<sup>a</sup> Guifang Dong\*,<sup>a</sup> Lian Duan<sup>a</sup>Received 00th January 2014,  
Accepted 00th January 2014

DOI: 10.1039/x0xx00000x

www.rsc.org/

We demonstrate a solution method of Marangoni effect-controlled oriented growth (MOG) to fabricate highly oriented crystals of 6, 13-bis(triisopropylsilylethynyl) pentacene (TIPS pentacene) on Si/SiO<sub>2</sub> substrate. Based on the Marangoni effect induced by mixed solvent system, large area aligned ribbon crystals can be achieved, covering over 60% on 4 cm × 1 cm Si/SiO<sub>2</sub> substrates. We investigated the growth mechanism of the MOG method and find that the correct choice of solvents and appropriate solvent ratio are in favor of aligned crystal growth. With the ribbon crystals of TIPS pentacene, top-contact organic field-effect transistors are fabricated. The optimal device exhibits field-effect mobility of  $0.70 \pm 0.22 \text{ cm}^2 \text{ V}^{-1} \text{ s}^{-1}$  and on/off ratio of  $10^5$ . The MOG method, which is potential to be used in batch production and is featured by easy control of crystal growth using non-contact forces, will benefit the development of low-cost, high-performance, organic semiconductor device.

## 1. Introduction

Organic field-effect transistors (OFETs) are of potential importance for electronic applications such as flexible circuits<sup>1</sup>, display backplanes<sup>2</sup> and sensors<sup>3-5</sup> due to low cost, chemical versatility and solution processability over their inorganic counterparts. High-crystalline OFETs have been attracting enormous attention because of their higher mobility and better environmental stability than the amorphous and polycrystalline OFETs. However, it is difficult to achieve highly aligned crystals of organic semiconductors owing to their preferential three-dimensional growth tendency. Several groups have developed solution processing techniques including external induced methods such as rubbing alignment,<sup>6</sup> magnetic alignment<sup>7</sup> and meniscus-guided coating methods such as zone casting<sup>8</sup> and dipcoating.<sup>9</sup> Besides, solution-shearing,<sup>10</sup> droplet-pinned crystallization,<sup>11</sup> electrostatic spray deposition,<sup>12</sup> slot-die coating,<sup>13</sup> volatilize-controlled deposition<sup>14</sup> are also used to align organic crystals. Despite the above methods which usually need special equipment, crystal alignment can also be achieved using non-contact, built in forces including gravitational force during dip-coating and drop casting on tilted substrates,<sup>15-17</sup> etc. Most of these methods are free of complex equipment, and crystal growth mechanism can be investigated without the interference of external forces or fields. The Kilwon Cho group reported the fabrication of one-dimensional crystal arrays of triisopropylsilylethynyl pentacene (TIPS pentacene) via simple drop casting on a tilted substrate and the crystal arrays are resulted from the directed organization of the  $\pi$ -conjugated molecules.<sup>17</sup> However, the coverage of the micro ribbons was less than 25% according to their results and it was a long time for the droplets to evaporate. Moreover, the thickness of the crystals (200-800 nm) was larger for OFET fabrication (usually the thickness of the semiconductor used in OFET is around 50 nm). Therefore, a quick and simple technology

should be developed to fabricate crystals with smaller thickness and better coverage which are more appropriate for OFET fabrication. This purpose implies reducing the amount of solution on the substrate and eliminating the coffee ring effect.

Based on the consideration above, we employed a large-area-compatible deposition technique, Marangoni effect-controlled oriented growth (MOG) and succeeded in preparing TIPS pentacene ribbon crystals on substrates within several minutes at room temperature. It should be noted that the TIPS pentacene crystals are highly oriented and the coverage on substrates is over 60%. In our approach, substrates with hydrophilic surfaces were immersed in solution and then partially pulled out (with the bottom of the substrate in the solution to pin the lower contact line). The amount of the solution in the liquid membrane was far less than in the droplets, leading to much thinner TIPS pentacene crystals. What's more, the thickness of ribbon crystals can be tuned by varying the solution concentration. As for the solvent selection, a mixed solution system composed by toluene and carbon tetrachloride was applied in the experiment. Compared with carbon tetrachloride, toluene has higher boiling point and lower surface tension. (Table S1) The mixed solution system could generate a Marangoni flow with a direction opposite that of the convective flow, resulting in uniform crystals alignment.<sup>18, 19</sup> In the previous reports the approach was only demonstrated with ink-jet printing and we succeeded in applying the approach to the MOG method. Besides, the evaporate rate can be adjusted by changing the ratio of the composition of the solvent mixture. Under optimum condition, the devices on the basis of the aligned TIPS pentacene crystals exhibited field-effect mobility of  $0.70 \pm 0.22 \text{ cm}^2 \text{ V}^{-1} \text{ s}^{-1}$  and on/off ratio of  $10^5$ , which are impressive values for the self-organized  $\pi$ -conjugated molecules derived from solution-processed methods. The MOG method offers a facile route for mass producible fabrication of high-quality semiconductor crystals.

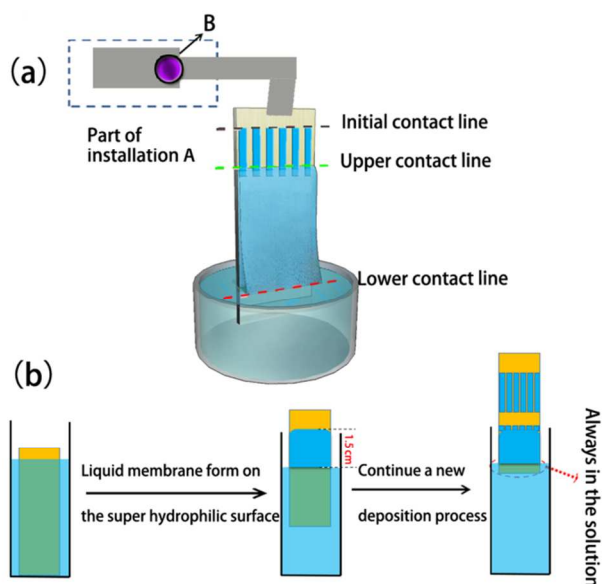


**Fig 1.** a) Schematic of the MOG system (not drawn to scale). By turning the knob B, the substrate could rise and fall quickly. b) Schematic steps of the MOG method.

## 2. Experimental Section

### 2.1. Materials and Surface Modification

Triisopropylsilylethynyl pentacene (TIPS pentacene) was purchased from Sigma-Aldrich and used without further purification. For the growth of TIPS pentacene crystals and the fabrication of the OFETs, highly doped n-type silicon wafers ( $<0.02 \Omega/\text{cm}$ ) each with a 300-nm thermally grown silicon dioxide were used as the substrates. In order to achieve super hydrophilic surfaces, the silica wafers were cleaned in a Piranha solution (70 vol %  $\text{H}_2\text{SO}_4$ , 30 vol %  $\text{H}_2\text{O}_2$ ) for 60 minutes at  $100^\circ\text{C}$ .

### 2.2. Solution Preparation and Crystal Deposition

The structure and function of the installation A in Fig 1(a) can help the substrate quickly move up and down. It should be noted that all the crystal growth procedure could also be fulfilled by manual operation, the purpose to use a special installation is to improve the precision (reliability and reproducibility) of the MOG method. The upper part of the substrate could be fixed to the installation A, by turning the knob B, the substrate could rise and fall quickly. The solutions for fabricating TIPS pentacene crystals were prepared by dissolving TIPS pentacene in a mixed solvent system composed by toluene and carbon tetrachloride (50 vol % toluene, 50 vol % carbon tetrachloride). The schematic steps were revealed in Fig 1(b). First, substrates with hydrophilic surfaces were immersed in the mixed solution for seconds and then partially pulled out of the solution by 1.5 cm (with the bottom of the substrate in the solution to pin the lower contact line). Consequently, the surface would be covered with a thin layer of the liquid (named liquid membrane) because of viscous forces on the super hydrophilic surface. As the solvent evaporated, the upper contact line of the liquid membrane spread down the substrate and the lower contact line remained pinned. Finally, ribbon-shaped, centimeter-long, micrometer wide and highly aligned crystals could be formed on  $\text{Si}/\text{SiO}_2$  substrates. If the

substrate was long enough, we could continually pull the substrate again by 1.5 cm to begin a new deposition process (always maintain the bottom of the substrate in the solution to pin the contact line). It should be noted that if the pulled distance was too long (longer than 1.5 cm), the alignment may get worse for the extra length out of 1.5 cm.

### 2.3. Characterization

The optical microscopy (OM) images were obtained using an optical microscope (BX51M, Olympus) and the polarized optical microscopy (POM) images were obtained using a polarized optical microscope (Nikon LV100POL). All POM images were recorded under cross-polarization with a constant polarizer angle. Grazing-incidence X-ray diffraction (GIXRD) measurements in the  $\theta/2\theta$  mode were performed using the synchrotron source at the 1W1A beamline of the Beijing Synchrotron Radiation Facility (BSRF) in China.

### 2.4. Fabrication of the OFETs

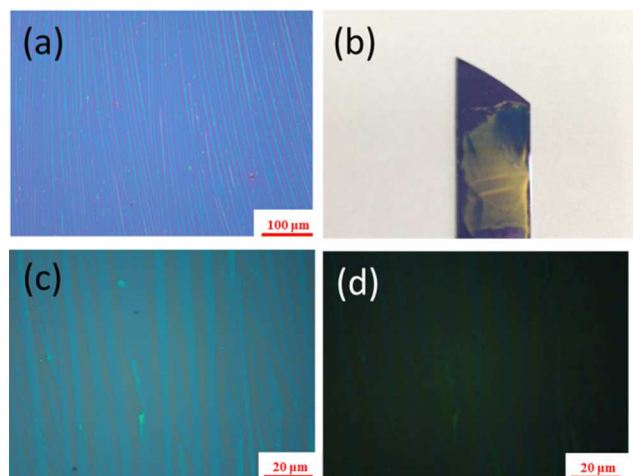
FETs with top-contact structures were fabricated using heavily doped n-type Si wafers as gate electrodes, with a 300 nm-thick thermally oxidized  $\text{SiO}_2$  layer as the gate dielectric. After the modification of  $\text{SiO}_2$  surface, TIPS pentacene crystals were formed by MOG method and used as the semiconductors. The source and the drain electrodes were Au thin films (50 nm) deposited by a conventional evaporation method with a metal mask. The electrical properties of the transistors were characterized by measuring their output and transfer curves (Keithley 4200) under ambient conditions. The average field-effect mobility ( $\mu$ ) of the FET devices was calculated in the saturation region by plotting the square root of the drain current ( $I_{\text{sd}}$ ) versus the gate voltage ( $V_g$ ) using the following equation:  $I_{\text{ds}} = \frac{WC_i}{2L} \mu (V_g - V_{\text{th}})^2$  where  $C_i$  ( $1.02 \times 10^{-8} \text{ F cm}^{-2}$ ) is the

unit area capacitance of the dielectric layer. The channel length was  $60 \mu\text{m}$  and the channel width was confirmed to be the sum of the

width of the crystals connecting the source and drain electrodes, which was approximately 500  $\mu\text{m}$  (the width of the electrode pattern was 800  $\mu\text{m}$ )

### 3. Results and Discussion

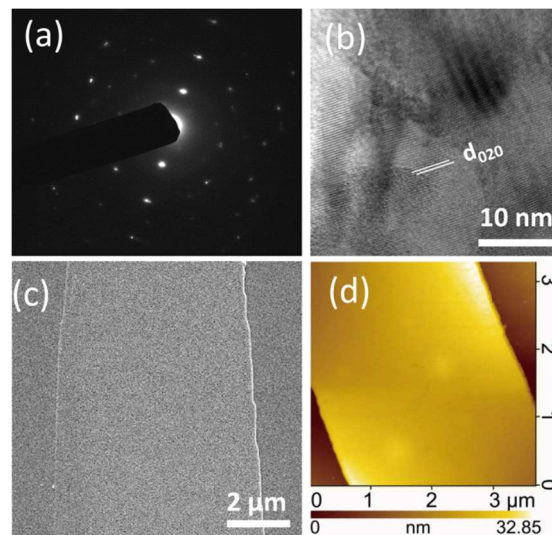
#### 3.1 The Characterizations of TIPS Pentacene Crystals.



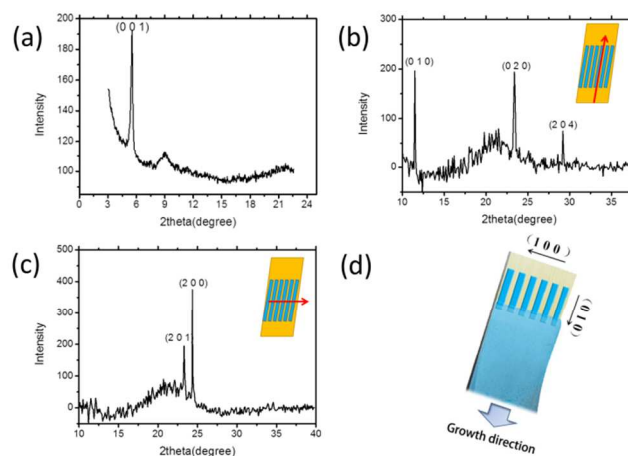
**Fig 2.** (a) Microscope image of TIPS pentacene crystals. (b) Picture of the substrate covered with TIPS pentacene crystals. (c) POM image of TIPS pentacene ribbon crystals. (d) POM image of TIPS pentacene ribbon crystals (we rotated the polariscope analyzer by 45° from panel c)

Fig 2a showed the microscope image of TIPS pentacene crystals, the crystals were ribbon-like and the length ranged from hundreds of micrometers to several millimeters. As was exhibited in Fig 2b, most area of the surface was covered with TIPS pentacene crystals. Fig 2 (c) and 2 (d) were the POM images of the crystals. The crystals showed the same color and brightness between crossed-polarizers. Besides, Transmission Electron Microscope (TEM), Atomic Force Microscopes (AFM), and Scanning Electron Microscope (SEM) test method were used in order to further investigate the crystallinity of the ribbon crystals (Fig 3). It was signified that the crystals were ordered in inner structure and the selected area electron diffraction (SAED) pattern generated by TEM at the non-overlapping regions showed the crystals were high-crystalline. The High Resolution TEM image of TIPS pentacene, Fig 3(b), exhibited the  $\pi$ - $\pi$  stacking distance of 3.3 Å, which was coincident with common TIPS pentacene crystals. Accordingly, we concluded that high quality TIPS pentacene crystals have been formed on the Si/SiO<sub>2</sub> substrate by this MOG method.

Out-of-plane X-ray diffraction (XRD) was carried out to confirm the crystalline structure of the crystals. As shown in Fig 4(a), a diffractive peak at  $2\theta=5.54^\circ$  was observed, corresponding to an inter-planar distance of 16.01 Å, which was attributed to the (001) diffraction of TIPS-pentacene crystal. We could conclude that the crystals arranged with c axis perpendicular to the substrate with TIPS pentacene molecules oriented with  $\pi$ - $\pi$  stacking parallel to the substrate.<sup>8, 14, 17</sup> Another result that supported the conclusion was the AFM test (see Fig S1 of the Supporting Information) near the border of the crystals, the height of the step was 1.70 nm that corresponded to the c-axis length of the TIPS pentacene molecules.



**Fig 3.** (a) SAED patterns of TIPS pentacene crystal, indicating high-crystallinity; (b) High resolution transmission electron microscopy (HRTEM) image of TIPS pentacene; (c) SEM image of TIPS pentacene ribbon crystals; (d) AFM image of TIPS pentacene ribbon crystals.



**Fig 4.** (a) Out-of-plane XRD patterns for the TIPS pentacene crystals (b) In-plane XRD patterns for the TIPS pentacene crystals when the X-ray direction was along the crystal growth direction (c) In-plane XRD patterns for the TIPS pentacene crystals when the X-ray direction was perpendicular to the crystal growth direction. (d) Schematic representation of the self-assembly of TIPS pentacene crystals

We also investigated the crystal anisotropic properties by using in-plane XRD with the X-ray parallel to the surface of crystal at a grazing angle (0.3°). When the X-ray direction was along the ribbon crystal growth direction, the XRD patterns (Fig 4(b)) showed obvious peaks at 11.54° and 23.40° respectively. These strong diffractive peaks could be attributed to the (010) and (020) diffraction of TIPS pentacene crystal, indicating that the crystal growth was along the b-axis direction. From Bragg's law  $2d\sin\theta = n\lambda$ ,  $\lambda=1.5480$  Å, the peak at 23.40° corresponded to a  $\pi$ - $\pi$  stacking distance of 3.8 Å. The appearance of the diffraction provided a supplementary evidence for the in-plane orientation of TIPS pentacene array. When the substrate was rotated by 90° (Fig 4(c)), the (010) and (020) diffraction disappeared, a strong peak at  $2\theta = 24.36^\circ$  was observed instead, and this peak was corresponding to the (200) plane. It should be noted that another peak at  $2\theta = 23.30^\circ$  was also presented and we contributed it to the (201) plane. It was due to

a metastable orientation of the TIPS pentacene molecules (with different angles of tilt) and this phenomenon often occurred in solution processed situations.<sup>8</sup> Both peaks indicated that the crystal growth direction was perpendicular to the a-axis direction. It deserved to be mentioned that the anisotropic properties of the crystal fabricated by MOG method was different from our previous work using the VOG method<sup>14</sup>. Even for the same molecule, if the fabrication method is different, the crystal anisotropic properties may be different.<sup>8,20</sup>

Based on the above analysis, we could conclude that the long axis of the ribbon crystal was along the b-axis direction and the  $\pi$ - $\pi$  stacking of TIPS-pentacene molecules was parallel to the substrate. The crystals were well-ordered, which favored carrier transportation along b axis. A visual schematic representation of the self-assembly of TIPS pentacene molecules was included in Fig 4(d).

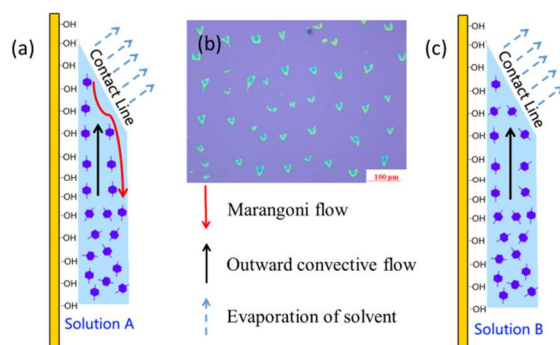


Fig 5. (a) Schematic illustration of TIPS Pentacene self-organization when applied the solution A (50 vol % toluene, 50 vol % carbon tetrachloride). (b) Microscope image of TIPS pentacene crystals from the mixed solution composed by toluene and isopropanol (50 vol % toluene, 50 vol % isopropanol). (c) Schematic illustration of TIPS Pentacene self-organization when applied the solution B (50 vol % toluene, 50 vol % isopropanol).

### 3.2 Mechanism Analysis of TIPS Pentacene Self-organization in MOG Method

The evaporation behavior during the drying process plays a vital role in controlling the crystal morphology and the alignment of crystals. A ring of solute that marks the border of the droplet is commonly observed in most of solution process, resulting from well known “coffee-stain” effect described by Petsi and Deegan.<sup>21, 22</sup> When the contact line is pinned during drying, the liquid membrane has a fixed contact area so a capillary flow of the solvent occurs from under the contact line to the contact line to replenish the evaporation loss, and this flow transports the solutes to its border. This effect results in a heterogeneous distribution of solute molecule, which is adverse to device performance. Therefore, our approach to improving the homogeneity involves fabricating from a mixed-solvent system to reduce the coffee ring effect. Our approach makes use of the evaporation-induced flow, in particular the convective and Marangoni flows that occur during drying. The Marangoni flow is induced by the surface tension gradient between the contact line and the interior of the liquid membrane from regions with low surface tension to regions with high surface tension. The convective flow that transports the solute to the contact line can be counter balanced or enhanced, depending on the direction of the Marangoni flow. For the MOG method, the two solvents in the solvent mixture should have different boiling points and surface tension. In this experiment, the carbon tetrachloride was the low boiling point (high evaporation rate) solvent with high surface tension while the toluene was the high boiling point (low evaporation rate) solvent with low surface

tension. Since the evaporation at the contact line was much faster than at the interior region of the liquid membrane, as drying proceeds, the solvent composition at the contact line shifted toward a higher fraction of toluene than the interior of the liquid membrane. Thus the surface tension at the contact line of the liquid membrane was relatively lower than that in the interior region because of the low surface tension of toluene. As shown in Fig 5(a), this surface tension gradient generated a Marangoni flow along the liquid membrane surface from the contact line to the interior region that counter balanced the convective flow and induced a recirculation flow in the liquid membrane, which resulted in the formation of self-aligned crystals of TIPS pentacene. This result is similar to the previous reports for self-organization of ink-jet-printed TIPS pentacene in a drying droplet.<sup>19</sup> In order to confirm the effect of the Marangoni flow, we compared the crystallization behavior of the solvent mixture with that of a single solvent. It's shown in Fig S2 that for the crystals fabricated from the solvent mixture, the crystals grew almost in the same direction both in the nucleation process and in the steady growth process. However, for the single solvent system, the crystals grew without orientation. Furthermore we used the mixed solvent composed by toluene and isopropanol (50 vol % toluene, 50 vol % isopropanol) to apply the MOG method and the microscope image of the achieved TIPS pentacene crystals was shown in Fig 5(b). It's obvious that the morphology of the achieved crystals was similar to the coffee ring-like crystals. Although the boiling point of isopropanol was lower than toluene, the surface tension of the two solvents were approximate (see Table S1), thus the Marangoni flow can't be generated to counterbalance the convective flow. (see Fig 5(c)).

The evaporation behavior also involves the evaporation rate of the solvent which can be controlled by adjusting the solvent composition. Three different solvent compositions were adopted in our approach and the correlative microscope images of the crystals from different solution were shown in Fig S3 of the Supporting Information (a. 75 vol % toluene, 25 vol % carbon tetrachloride b. 50 vol % toluene, 50 vol % carbon tetrachloride c. 25 vol % toluene, 75 vol % carbon tetrachloride). When the volume fraction of the toluene was 75%, highly aligned ribbon crystals can be achieved, however some spherulites or branched crystals could be observed across one ribbon crystal (labeled in Fig S3(a)). As the volume fraction of the toluene decreased to 50%, ribbon crystals of high alignment were achieved and few spherulites or branched crystals observed in the view. (Fig S3(b)) When we further decreased the volume fraction of the toluene to 25%, the variation of crystal orientation became obvious. (Fig S3(c)) The transition of the crystalline morphology is explained here. As we know, TIPS pentacene molecules tended to crystallize along the direction of the concentration gradient, which was accordant to the contact line declining direction<sup>20</sup>. That was why the MOG method could be used to align organic molecules. When the evaporate rate was low enough, the concentration gradient should be indistinctive. As a result, for a certain time, no preferential direction existed for the growth of TIPS pentacene crystals, and spherulites or branched crystals formed. As the volume fraction of the toluene was decreased, the evaporate rate increased, the concentration gradient became remarkable, and the crystals tended to grow along the contact line receding direction. An oriented crystalline array with high quality was fabricated. However when the evaporate rate was too high, the crystalline alignment became more irregular. We attributed the phenomenon to the too fast crystallization of TIPS-pentacene molecules, which may induce undesired crystalline alignment.

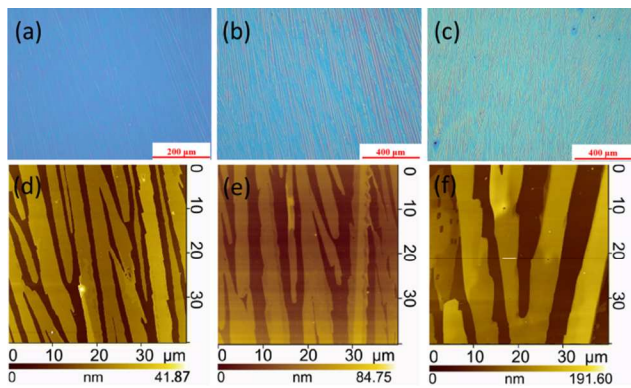


**Fig 6** Optical microscope images (a-c) and AFM images (d-f) of TIPS pentacene crystals at different solution concentrations. (a, d @1g/L b, e @2g/L c, f @5g/L)

Taking it into account that the solution concentration was also an important factor that may effect on the drying-mediated self-assembly of crystal, solutions of different concentrations from 1 g/L to 5 g/L were prepared. Fig 6 (a)-(c) show the optical microscope images of TIPS pentacene crystals grown from different solutions. When the concentration was 1 g/L, highly oriented TIPS pentacene ribbon crystals formed on the substrate. As we increased the concentration to higher than 2 g/L, the width of crystals got larger and the surface got rough obviously. AFM images of the crystals were demonstrated in Fig 6(d)-(f). With the solution concentration varying from 1 to 5 g/L, the average thickness of the crystal increased from 16.5 to 76.2 nm, while the Root Mean Square (RMS) value increased from 0.343 to 1.01 nm. (The RMS value was obtained from an area of  $1 \times 1 \mu\text{m}$  of complete crystal surface)

In our opinion too much nuclei at the contact line would impede the continuous growth of an oriented crystalline array, resulting in the stacking of disordered multilayer. On the basis of these results, we could conclude that the Marangoni effect was essential for the MOG process of TIPS pentacene molecules. Self-aligned TIPS pentacene crystals were successfully produced when there was a recirculation flow that was induced by a Marangoni flow in the direction opposite to the convective flow. In order to obtain organic semiconductor crystals with highly ordered molecular structure via the MOG process, a proper solvent composition and solution concentration were also desirable which were respectively responsible for the evaporation rate and density of nuclei at the contact line.

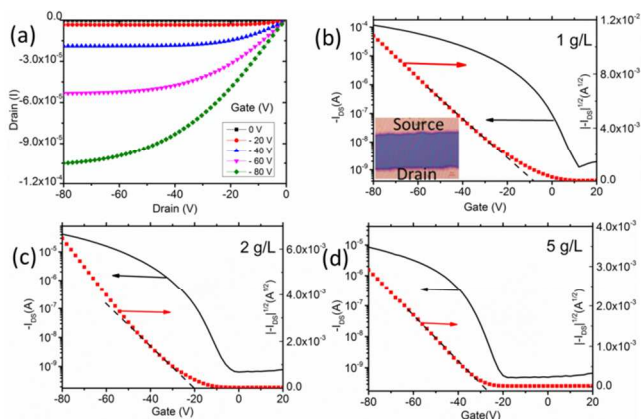


**Fig 7** OFET characteristics images of the TIPS pentacene with source-drain bias parallel to the crystal growth direction. (a) the output characteristic curve of the OFETs. (b) the transfer characteristic curve of the OFETs (@solution concentration of 1 g/L) (c) the transfer characteristic curve of the OFETs (@solution concentration of 2 g/L) (d) the transfer characteristic curve of the OFETs (@solution concentration of 5 g/L)

### 3.3 Characteristics of Field Effect Transistors

To evaluate the electrical characteristics of these ribbon crystals prepared by MOG method on bare  $\text{SiO}_2/\text{Si}$  substrate (@solution concentration of 1 g/L), top-contact bottom-gate field-effect transistors were fabricated. From 13 devices performed, the field-effect mobility extracted from the transfer characteristics was  $0.70 \pm 0.22 \text{ cm}^2 \text{ V}^{-1} \text{ s}^{-1}$  and on/off ratio of  $10^5$ . (Fig 7 a,b). As for the hysteresis in Fig S4, we suggested that trapping at the localized states at the  $\text{SiO}_2\text{-OH}/\text{semiconductor}$  interface and the grain boundaries caused instability of the OFETs. Our studies focusing on overcoming these drawbacks are underway.

The largest field-effect mobility was obtained for the crystals prepared at the lowest concentration (1 g/L). Better alignment of the molecules was visible from the AFM image in Fig 6 (d), which in combination with the absence of defects resulted in a high mobility in the direction of the crystal growth. As the solution concentration increased from 1 g/L to 5 g/L, a maximum field-effect mobility declining from  $0.92$  to  $0.04 \text{ cm}^2 \text{ V}^{-1} \text{ s}^{-1}$  was observed. Other differences in the transfer characteristics were the increase in threshold voltage and decrease in  $I_{\text{on}}/I_{\text{off}}$ . When the solution concentration was higher than 2 g/L, the threshold voltage moved from  $-8.5 \text{ V}$  to  $-27.1 \text{ V}$  and the  $I_{\text{on}}/I_{\text{off}}$  dropped to  $10^4$  (Fig 7 c,d). These differences can be explained by the thickness of the crystals prepared at different concentrations. Due to a top contact configuration, when the thickness of the crystal was large, the induced charges should overcome a long distance from the semiconductor/dielectric interface to the source-drain electrodes, resulting in a much lower on current ( $I_{\text{on}}$ ), thus a decrease in on/off ratio ( $I_{\text{on}}/I_{\text{off}}$ ) was observed. Besides, a thick semiconductor can transport current between source and drain when the transistor channel was not completely filled with charges at the semiconductor/dielectric interface. This increased the value for  $V_{\text{th}}$ . The above result was consistent with the previous report<sup>23</sup> that thinner crystals/films gave rise to better performance of OFETs.

### 4. Conclusions

In conclusion, we demonstrated an effective MOG method to deposit large area high-crystalline crystals of organic semiconductor materials. Based on the Marangoni effect, TIPS pentacene molecules were quickly self-organized with a highly ordered crystalline structure on  $\text{SiO}_2$  surface. The MOG method is based on the directed organization of the  $\pi$ -conjugated molecules using non-contact, built in forces and does not require any post-processing. In addition, growth mechanism of TIPS pentacene crystals was discussed with Marangoni effect. On the basis of the TIPS pentacene crystal, top-contact organic field-effect transistors with field-effect mobility of  $0.70 \pm 0.22 \text{ cm}^2 \text{ V}^{-1} \text{ s}^{-1}$  and on/off current ratio of  $10^5$  were achieved. This work shows that MOG method is a potential technology for industrial applications of organic semiconductors.

### Acknowledgements

The authors thank the National Natural Science Foundation of China (No. 61177023, 51173096, and 61474069). A portion of this work is based on the data obtained at 1W1A, BSRF. The authors gratefully acknowledge the assistance of the scientists of the Diffuse X-ray Scattering Station during the experiments.

## Notes and references

<sup>a</sup> Key Laboratory of Organic Optoelectronics and Molecular Engineering of Ministry of Education, Department of Chemistry, Tsinghua University, Beijing, 100084 (P. R. China). Fax: (86)010-62782287; Tel: (86)010-62782287; E-mail: donggf@mail.tsinghua.edu.cn;

<sup>†</sup> Electronic Supplementary Information (ESI) available: Table S1. A summary of the physical parameters of the solvents used in this work. Fig S1. AFM images of the solution grown crystals of TIPS pentacene; Fig S2. Microscope image of TIPS pentacene crystals from different solvent systems; Fig S3. Microscope image of TIPS pentacene crystals from the mixed solution with different solvent composition; Fig S4. Hysteresis behavior of OTFT devices based on TIPS pentacene crystals.

- 1 V. Subramanian, P. C. Chang, J. B. Lee, S. E. Molesa, and S. K. Volkman, *IEEE T Compon Pack T.*, 2005, **28**, 742-747.
- 2 T. Someya, A. Dodabalapur, J. Huang, K. C. See, and H. E. Katz, *Adv Mater.*, 2010, **22**, 3799-3811.
- 3 S. C. B. Mannsfeld, B. C. K. Tee, R. M. Stoltenberg, C. V. H-H. Chen, S. Barman, B. V. O. Muir, A. N. Sokolov, C. Reese, and Z. N. Bao, *Nat Mater.*, 2010, **9**, 859-864.
- 4 H. Y. Zhao, G. F. Dong, L. Duan, L. D. Wang and Y. Qiu, *J Phys Chem C.*, 2013, **117**, 58-63.
- 5 M. Ramesh, Y. R. You, M. Shellaiah, M. C. Wu, H. C. Lin and C. W. Chu, *Org Electron.*, 2014, **15**, 582-589.
- 6 B. J. Jung, N. J. Tremblay, M. L. Yeh and H. E. Katz, *Chem. Mater.*, **2011**, **23**, 568-582.
- 7 I. O. Shklyarevskiy, P. Jonkheijm, N. Stutzmann, D. Wasserberg, H. J. Wondergem, P. C. M. Christianen, A. P. H. J. Schenning, D. M. d. Leeuw, Z. Tomovic, J. S. Wu, K. Mullen and J. C. Maan, *J. Am. Chem. Soc.*, **2005**, **127**, 16233-16237
- 8 Y. J. Su, X. Gao, J. G. Liu, R. B. Xing and Y. C. Han, *Phys Chem Chem Phys.*, 2013, **15**, 14396-14404.
- 9 R. Z. Rogowski, A. Dzwilewski, M. Kemerink and A. A. Darhuber, *J. Phys. Chem. C*, 2011, **115**, 11758-11762.
- 10 Y. Diao, B. C. K. Tee, G. Giri, J. Xu, D. H. Kim, H. A. Becerril, R. M. Stoltenberg, T. H. Lee, G. Xue, S. C. B. Mannsfeld and Z. N. Bao, *Nat. Mater.*, 2013, **12**, 665-671.
- 11 H. Li, B. C. K. Tee, G. Giri, J. W. Chung, S. Y. Lee and Z. Bao, *Adv. Mater.*, 2012, **24**, 2588-2591.
- 12 N. Onojima, H. Saito and T. Kato, *Org. Electron.*, 2013, **14**, 2406-2410.
- 13 J. J. Chang, C. Y. Chi, J. Zhang and J. S. Wu, *Adv. Mater.*, 2013, **25**, 6442-6447.
- 14 H. Y. Zhao, D. Li, G. F. Dong, L. Duan and L. D. Wang, *Langmuir* 2014, **30**, 12082-12088.
- 15 L. Li, P. Gao, K. C. Schuermann, S. Ostendorp, W. Wang, C. Du, Y. Lei, H. Fuchs, L. De Cola, K. Muellen and L. Chi, *J. Am. Chem. Soc.*, 2010, **132**, 8807-8809.
- 16 T. Uemura, Y. Hirose, M. Uno, K. Takimiya and J. Takeya, *Appl. Phys. Express*, 2009, **2**, 111501.
- 17 W. H. Lee, D. H. Kim, Y. Jang, J. H. Cho, M. Hwang, Y. D. Park, Y. H. Kim, J. I. Han and K. Cho, *Appl. Phys. Lett.*, 2007, **90**, 132106.
- 18 H. Hu and R. G. Larson, *J Phys Chem B.*, 2006, **110**, 7090-7094.
- 19 J. A. Lim, W. H. Lee, H. S. Lee, J. H. Lee, Y. D. Park and K. Cho, *Adv. Funct. Mater.*, **2008**, **18**, 229-234
- 20 D. H. Kim, D. Y. Lee, H. S. Lee, W. H. Lee, Y. H. Kim, J. I. Han, K. Cho, *Adv. Mater.*, 2007, **19**, 678-682.
- 21 A. J. Petsi and V. N. Burganos, *Phys. Rev. E.*, 2006, **73**, 041201.
- 22 R. D. Deegan, O. Bakajin, T. F. Dupont, G. Huber, S. R. Nagel and T. A. Witten, *Nature.*, 1997, **389**, 827-829.
- 23 Y. Yuan, G. Giri, A. L. Ayzner, A. P. Zoombelt, S. C. B. Mannsfeld, J. Chen, D. Nordlund, M. F. Toney, J. Huang and Z. Bao, *Nat. Commun.*, 2014, **5**, 3005.